



University of Dundee

Design, simulation and implementation of a PID vector control for EHVPMSM for an automobile with hybrid technology

Adeoye, Adeyinka O.M.; Oladapo, Bankole I.; Adekunle, Adefemi A.; Olademeye, Ayamolowo J.; Kayode, Joseph F.

DOI:

[10.1016/j.jmrt.2017.07.005](https://doi.org/10.1016/j.jmrt.2017.07.005)

Publication date:
2019

Licence:
CC BY-NC-ND

Document Version
Publisher's PDF, also known as Version of record

[Link to publication in Discovery Research Portal](#)

Citation for published version (APA):

Adeoye, A. O. M., Oladapo, B. I., Adekunle, A. A., Olademeye, A. J., & Kayode, J. F. (2019). Design, simulation and implementation of a PID vector control for EHVPMSM for an automobile with hybrid technology. *Journal of Materials Research and Technology*, 8(1), 54-62. <https://doi.org/10.1016/j.jmrt.2017.07.005>

General rights

Copyright and moral rights for the publications made accessible in Discovery Research Portal are retained by the authors and/or other copyright owners and it is a condition of accessing publications that users recognise and abide by the legal requirements associated with these rights.

- Users may download and print one copy of any publication from Discovery Research Portal for the purpose of private study or research.
- You may not further distribute the material or use it for any profit-making activity or commercial gain.
- You may freely distribute the URL identifying the publication in the public portal.

Take down policy

If you believe that this document breaches copyright please contact us providing details, and we will remove access to the work immediately and investigate your claim.



Available online at www.sciencedirect.com

jmr&t
Journal of Materials Research and Technology
www.jmrt.com.br



Original Article

Design, simulation and implementation of a PID vector control for EHVPMSM for an automobile with hybrid technology



Adeyinka O.M. Adeoye^a, Bankole I. Oladapo^{a,*}, Adefemi A. Adekunle^b, Ayamolowo J. Olademeyeji^c, Joseph F. Kayode^a

^a Mechanical and Mechatronics Engineering, Afe Babalola University, Ado-Ekiti, Nigeria

^b Mechanical and Mechatronics Engineering, Federal University Oye-Ekiti, Oye-Ekiti State, Nigeria

^c Electrical Computer Engineering, Afe Babalola University, Ado-Ekiti, Nigeria

ARTICLE INFO

Article history:

Received 5 February 2017

Accepted 20 July 2017

Available online 10 November 2017

ABSTRACT

This work proposes a Model design simulation and implementation of a novel engine of an Electric Hybrid Vehicle of Permanent Magnet Synchronous Motor (EHVPMSM) based on field oriented vector control. The experimental analysis was carried out using: automotive motor control MTRCKTSPS5604P, 3-Phase PMSM coded of a single Motor Control Kit with MPC5604P MCU and simulation with Simulink. Therefore, the direct torque control can be obtained by adjusting the magnitude and phase angle of the stator flux linkage to match the vector torque required by the load as fast as possible. This eradicates the stress of charging the vehicle battery. It automatically charges when it is connected to the main supply of the EHVPMSM. The electromagnetic torque can be increased from 0 Nm to 6.7 Nm in approximately 340 μ s. The response of speed transient was from –2100 rpm to +2100 rpm in 100 ms of 6.7 Nm torque limit. This is a novel way of conserving the energy consumption in a vehicle, which conserves space and weight and minimizes cost as it is simply done with low-cost materials. In this research, a new mathematical model is proposed for the direct and quadrature axis of the current to control the speed mechanism for the engine. Computer simulation ensures experimental validation of the system with a percentage error of 4.5%. The methodology employed to control the system was with the use of various sensors and software controller, this can be easily implemented in industry and institutional laboratory of learning.

© 2017 Brazilian Metallurgical, Materials and Mining Association. Published by Elsevier Editora Ltda. This is an open access article under the CC BY-NC-ND license (<http://creativecommons.org/licenses/by-nc-nd/4.0/>).

* Corresponding author.

E-mail: bankolyable@yahoo.com (B.I. Oladapo).

<https://doi.org/10.1016/j.jmrt.2017.07.005>

2238-7854/© 2017 Brazilian Metallurgical, Materials and Mining Association. Published by Elsevier Editora Ltda. This is an open access article under the CC BY-NC-ND license (<http://creativecommons.org/licenses/by-nc-nd/4.0/>).

1. Introduction

Due to the greater environmental and social awareness of this age, the use of alternatives for the traction of vehicles has experienced a growth in past years. Along the same line, there are already many manufacturers that deal with one or more models of hybrid vehicles in the market [1,2]. These hybrid vehicles combine a conventional internal combustion engine with an electric machine. This technology has been adopted because of the problems of weight, cost, performance and infrastructure [2,3]. The main axis of this study is to determine or establish a type of engine together with a control strategy that adapts to the needs and requirements of the electric engine hybrid vehicle. In recent years, more efficient alternating machines have been considered, the continuous ones; which are used for hybrid vehicles and the electric ones of average and great power [3,4]. Within the AC motors, those that have higher performance in terms of robustness are synchronous motors such as those of permanent magnets, rotor winding or switched reluctance [5]. For this reason, the present study will deal with the synchronous rotor winding machine with protruding poles and DC rotor excitation and the Electric Hybrid Vehicle of Permanent Magnet Synchronous Motor (EHVPM). The main difference is that in the case of the first machine, magnetic field is created in the rotor of the machine to the DC rotor excitation, which makes it fluctuate [6–8], while in the case of the novel EHVPM, the field created is constant as it is determined by the magnets mounted on the rotor and it is continuously constant. The control strategy used for both machines will be the vectorial control or field-oriented control (FOC) with a first stage in which the models will be implemented on Matlab/Simulink, and a subsequent second phase in which it is implemented on a configure automotive motor control MTRCKTSPS5604P and 3-Phase PMSM coded of a single Motor Control Kit with MPC5604P MCU. This device is mounted on a plate that forms part of a development kit and includes the studio software. The kit is designed for the control of motors with many blocks for the implementation of vector control as well as the generation of PWM pulses [8–10]. The use of vector control allows extrapolating the control technique of direct current motors to the field of the alternating motors; being able to decouple the mathematical model of the machine and control the components responsible for magnetic flow and drive torque independently. In this way, to control the composition of the pair, a control loop may be with a machine such as a WRSM machine [10–12]. There is a control measure on the permanent magnets, which is a result of the excitation current of the rotor. Hybrid vehicles that follow the 'Hybrid Synergy Drive' philosophy are the first in the world to rely on a fully active safety package electrical and electronic equipment, including power steering and the first braking by cable with a completely electrical system. ABS, EBD and VSC were also incorporated in it and ran with an electric circuit [10]. A central electronic brain coordinates these systems to create a perfect work together. This allows all active security systems and power steering to act as one in a dangerous situation. The synchronous motors are connected to the frequency of the source and the pole of the motor pair always rotating at the synchronous speed depending on the number of excited

machines. The stator of these motors uses alternating current (AC) and the rotors are fed with direct current (DC) [11–13]. However, the rotor magnetic field in synchronous motors positioned in rotor's need for the second source when provided with permanent magnets and thus PMSMs are obtained. Any current in the motor rotor copper losses is not a big deal. Also, the magnetizing current, which is the component of the stator current, increases the power coefficient of the motor. Therefore, this smaller engine design had the same strength as other engines and higher efficiency. This means that a high power is a desirable feature for vehicle and aircraft technology. In many applications of high torque and low speed, the PMSM is preferred but present a particular disadvantage for speed ranges above the nominal speed [12,13]. The fixed flux imposed by the magnets in the air gap makes the speed increase, the voltage induced in the windings increases very high above those allowed by the machine itself and the converter. To avoid this phenomenon, the field must be weakened in the air gap for high operating ranges of rated speed [14,15]. Numerous methods of the weakening of the field have been researched to solve this problem.

Hassan et al., Liu and Zhu and Qiao et al. [11,16,17] investigate a new direct torque control of a sensorless interior permanent magnet synchronous motor, which is based on a sliding method. The position and speed of the interior PMSM are calculated online based on active flux idea. In order to overcome large ripple content commonly found with direct torque, a torque/flux sliding mode controller was used.

Rong-Maw et al. and Guoyang et al. [18,19] introduce a robust PID control scheme for the PMSM using a genetic searching approach. A Genetic Algorithms (GAs) are powerful searching algorithms, which depend on natural genetics and mechanics of natural selection. They presents a mode switching control (MSC) system in discrete-time domain for precise and fast set-point tracking in servo systems dependent on control saturation of unknown disturbance.

Fayez and El-Sousy [20] adopt computed torque control for PMSM for an adaptive hybrid control system (AHCS) of a servo drive. The suggested AHCS in incorporating an auxiliary controller, which depend on the sliding-mode control of a recurrent radial basis function network (RBFN).

Recently Mahdi et al. and Shriwastava et al. [2,9] proposed a sensorless PMSM drive based on direct power control method. In order to calculate the rotor's speed and position of PMSM, a strong sensorless strategy was developed according to artificial neural network to reduce the cost of the driving the machine and increase accuracy. Also, an implementation of three level diode-clamped multilevel inverter using IGBT's fed for PMSM drive was proposed. Carrier based space vector pulse width modulation technique was used for the pulses for the inverters.

In early 2017, Mahmoud et al. [1] presents a novel speed monitor established on fuzzy logic system for speed sensorless control for PMSM. The switch function in the common Sliding Method monitor is substituted for a rule based fuzzy logic system.

All these brought about the motivation in this paper for further study of PMSM. The objectives of this research are to use the Vector Control Technique to improve the system

dynamic performance during parameter variation and the monitoring system which has high tracing performance. This is done by placing the stator current vector in a way that, the speeds above the nominal, a part of the flow associated with it is subtracted from the main flow imposed by the magnet maintaining the constant voltage in the terminals of the machine. Based on this technique, the selection of parameters is essential for extending power capacity above speed nominal. Also, we performed a comparative study between two possible solutions for the implementation of vector control over synchronous motors in a vehicles with hybrid technology for the permanent magnet motor and the winding rotor. This is to help achieve the best method to implement vector control on the EHVPMSM and the synchronous winding rotor using Simulink. These are check the speed and torque set points for the machines and perform of a technical-economic analysis on the systems.

2. Continuous magnet synchronous motor direct torque control

The basic principle of direct torque control is stator magnetic field between flow and momentum reference and a real value depending on the difference, the appropriate stator voltage vectors are selected. Permanent magnet synchronous motor is used if the magnetic flux is constant. At the moment control width modulation (PWM) comparator the necessity of using the current control circuit arises. For this reason, permanent magnet synchronous motors direct torque control. PWM current control is less parameter dependence than torque control and fast moment response [21]. Driver control used in complex structures is independent of the method and the control variables, the system's parameter dependence reduction becomes mandatory for the applicability of the system income. For this reason, the three-phase equations of the electric machine's process intensity can be lifted off by lowering the two parts current control for high dynamic performance of rotor flux reference system [16,17,22]. In the study below, direct and indirect vector control motor equations were used in reference system and permanent magnet. The mathematical model of the synchronous motor is given.

3. Theoretical equation of implementation for EHVPMSM

Stator magnetic flux vector, Ψ and the rotor magnetic flux vector, ψ is as shown in Fig. 1. Also, the rotor flux (dq) and the stator flux (xy) reference systems. Stator and rotor magnetic with the angle δ between the wings is the load angle. Δ is a constant load and does not change at the moment. In this case, the flow also rotates synchronously [10,17]. However, at different loads, δ changes. Here, the change in the rotation speed or δ of the stator current can be controlled, the increase in the moment can be controlled.

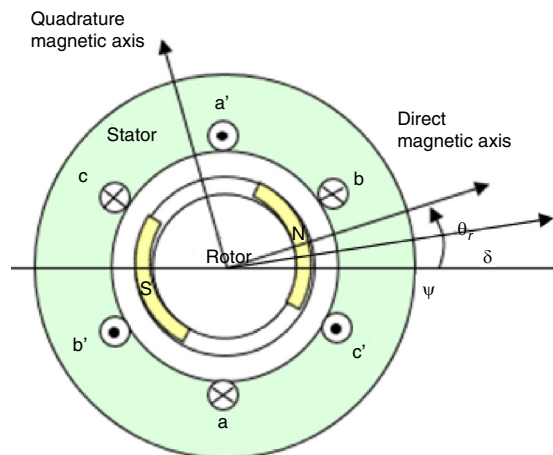


Fig. 1 – Space vector for stator fluxes in synchronous different reference for the systems.

The electrical equations for the block from Fig. 1 can be defined in terms of flux partial derivatives as the following equations:

$$V_a = \frac{\delta\phi}{\delta i_a} \frac{\delta i}{\delta t} + \frac{\delta\phi}{\delta \theta_r} \frac{d\theta_r}{dt} - M_s \left(\frac{di_b}{dt} + \frac{di_c}{dt} \right) + R_s i_a \quad (1)$$

$$V_b = \frac{\delta\phi}{\delta i_b} \frac{\delta i}{\delta t} + \frac{\delta\phi}{\delta \theta_r} \frac{d\theta_r}{dt} - M_s \left(\frac{di_a}{dt} + \frac{di_c}{dt} \right) + R_s i_b \quad (2)$$

$$V_c = \frac{\delta\phi}{\delta i_c} \frac{\delta i}{\delta t} + \frac{\delta\phi}{\delta \theta_r} \frac{d\theta_r}{dt} - M_s \left(\frac{di_a}{dt} + \frac{di_b}{dt} \right) + R_s i_c \quad (3)$$

where V_a , V_b , V_c are the voltages applied to the A, B, and C stator and i_a , i_b , i_c are the stator currents in each of the three phase windings of the motor. R_s is the resistance of each of the stator, M_s is the stator-stator mutual inductance and $\frac{\delta\phi}{\delta i_a}$, $\frac{\delta\phi}{\delta i_b}$, $\frac{\delta\phi}{\delta i_c}$ are the partial derivatives of flux linkage with respect to stator current in each of the three windings, $\frac{\delta\phi}{\delta \theta_r}$ is the partial derivative of flux linkage with respect to rotor angle.

The following equations are the functional equations for the PID control and the limiters of the EHVPMSM which flow through the PMSM motor and the dynamometer:

$$F(x) = x \cos 3x - 2x \sin 3x \quad (4)$$

$$F(x) = x \cos(3x - 2\pi/3) - 2x \sin(3x - 2\pi/3) \quad (5)$$

$$F(x) = x \cos(3x + 2\pi/3) - 2x \sin(3x + 2\pi/3) \quad (6)$$

$$F(x) = x \cos(4x + 2x) \cos(4x - 2\pi/3) - 3x \cos(4x + 2\pi/3) \quad (7)$$

$$F(x) = -x \sin(4x - 2x) \sin(4x - 2\pi/3) - 3x \sin(4x + 2\pi/3) \quad (8)$$

The block can automatically calculate the torque matrix from the flux information provided; see Eqs. (4)–(8), this results in Eq. (9) after simulation on the PID controlling system

$$F = P + I \frac{1}{s} + D \frac{N}{1 + N \frac{1}{s}} \quad (9)$$

3.1. Engine modelling and speed control for permanent magnet synchronous motor

The engine section is shown in Figs. 3 and 4, which show the different variables necessary for the mathematical model of the same mathematical equations used for the modelling of the motor, which are the classic ones of an asynchronous permanent magnet machine [19]. These, expressed directly in a rotor reference system which rotates at the speed of synchronism are as following:

$$\Psi_{sq} = L_{sd} i_{sq} \quad (11)$$

$$\Psi_{sd} = L_{sd} i_{sd} + \Psi_M \quad (10)$$

$$U_{sd} = R_s i_{sd} + \frac{d}{dt} \Psi_{sd} + \omega_r \Psi_{sd} \quad (12)$$

$$U_{sd} = R_s i_{sd} + \frac{d}{dt} \Psi_{sd} + \omega_r \Psi_{sd} \quad (13)$$

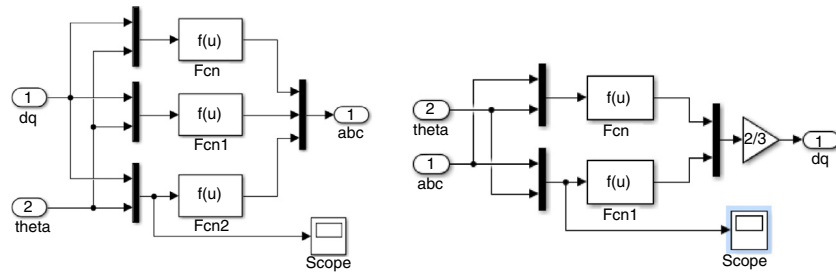


Fig. 2 – Block parameters that apply specified expression to input with a definition box.

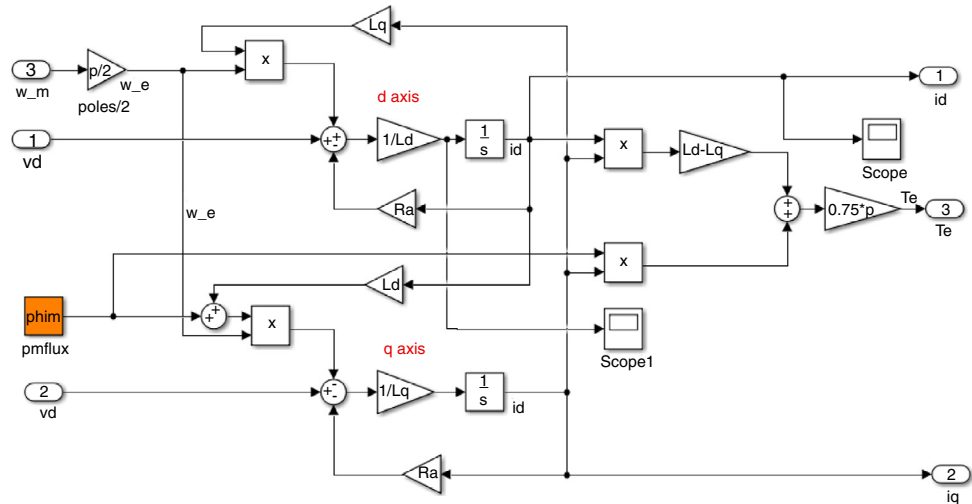


Fig. 3 – Simulation model of the functional PID vector control EHVPMSM drive.

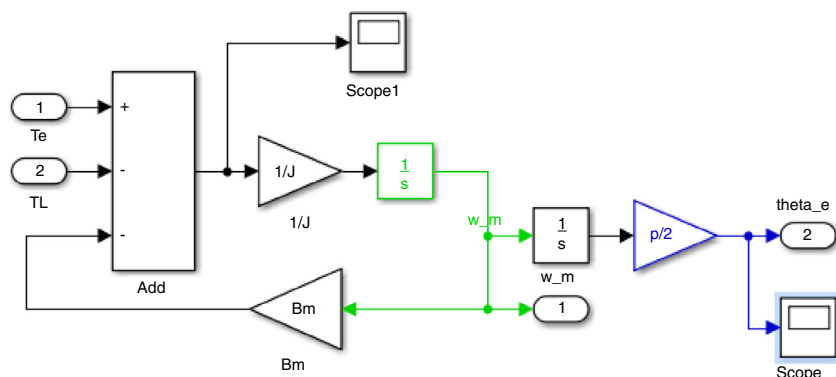


Fig. 4 – Simulation model of the functional PID speed control EHVPMSM drive.

The structural differences of permanent magnet synchronous motors, d and q axes have different inductance values, which can be express as the following equations. Combining the above equations result in Eqs. (12) and (13) which is express as:

$$T_e = \frac{3}{2}P(\psi_{sd}i_{sq} - \psi_{sq}i_{sd}) \quad (14)$$

$$T_e = \frac{3}{2}P[\psi_M i_{sq} - (L_{sq} - L_{sd})i_{sd}i_{sq}] \quad (15)$$

For PMPM, the direct and quadrature components of the inductances of the system are equal in field of expression. That is $L_{sd} = L_{sq}$ and $i_{sd} = i_{sq}$ which makes Eq. (15) becomes Eq. (16), which is the developed mathematical model equation.

$$T_e = \frac{3}{2}P[\psi_M i_{sq}] \quad (16)$$

From the model Eq. (16), the torque producing is along the quadrature-axis and it is directly proportional to the current product along the quadrature-axis with respect to time [14,20]. For maximum efficiency to be reached, the torque per ampere relationship should be increasing along the axis. This can be achieved by setting the direct-axis current to a constant value at all times. The rotor has d and q axis of different inductance values. Given in Eq. (15), the moment equation can be expressed more simply [14]. The expression is given by Eq. (16), which is derived from Figs. 1–4, which is the expression of the transformation made by the load angle. The trigonometric expressions are given in Eq. (8) to also obtained Eq. (17).

$$\begin{bmatrix} F_d \\ F_q \end{bmatrix} = \begin{bmatrix} \cos \delta & -\sin \delta \\ \sin \delta & \cos \delta \end{bmatrix} \begin{bmatrix} F_x \\ F_y \end{bmatrix} \quad (17)$$

from the equations above, ψ_{sd} is the voltage on the d -axis, ψ_{sq} is the voltage on the q axis, i_{sd} is the current on the d -axis, i_{sq} is the current on the q axis, R_s is the phase resistance of the stator windings, L_{sd} is the phase inductance of the stator windings, U_{sd} is the electric speed of the rotor and ω_r is the flow created by the permanent magnets of the machine [11–13]. It

will help for engine modelling and speed control and also for mechanical control of the machine.

3.2. Flux Orientation Speed Control

The method chosen for speed control for Flux Orientation Speed Control (FOC) aims to control the flow magnetic torque and the torque developed by the motor, by controlling the components d and q of the stator currents. To achieve this, with the information of the stator currents and the rotor angle, you can control the flow through the air gap as well as the pair developed by the machine in a very effective way. The main advantages of this method are its rapid response to changes in the load or variations in the speed reference as well as its minimum ripple in the developed pair. Fig. 5 shows a schematic of the designed speed controller and the experimental setup in Fig. 6.

4. Discussion

The implementation of the EHVPMSM is carried out using the synchronous 6-pole, 2 kW motor, three-phase inverter, voltage, current and rotor angle sensors and interface between physical system and computer: DSpace 1103 and various protection systems like fuses and PWM signal switches. All these equipment were calibrated and tested to check their precision and accuracy. The results obtained in these tests were highly reliable and favours the idea in view. Fig. 7 shows a general scheme of the assembly and the outline of the points of measurement of currents and voltages.

In this scheme, the applied control can be appreciated. Firstly, the reference to the actual engine speed; the error obtained was entered in a PI (proportional-integral) regulator from which we obtained the pair required because we had to develop the engine to get the required speed. Applying Eq. (13), this pair becomes the reference of the q component of the

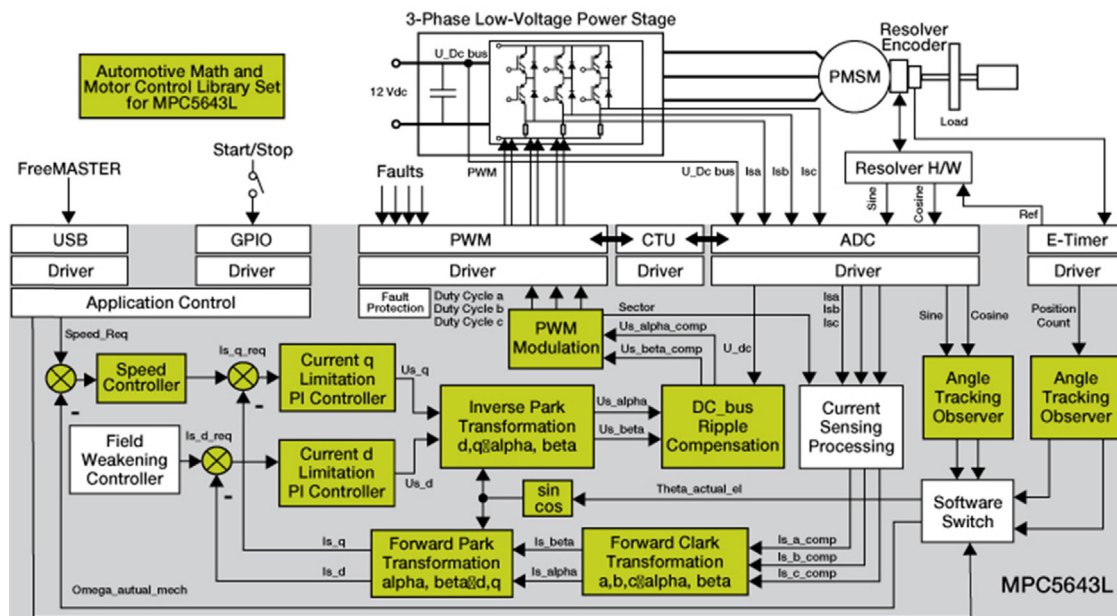


Fig. 5 – Schematic of the experimental setup of motor control algorithm of implemented drive for EHVPMSM.

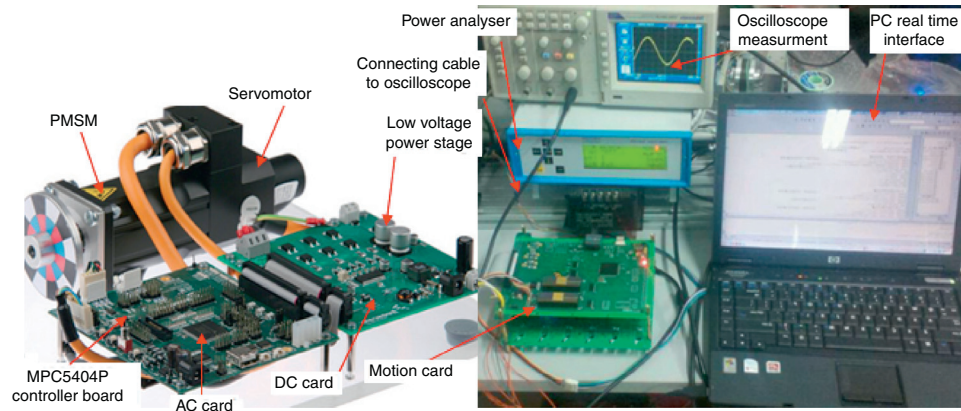


Fig. 6 – Experimental setup of the developed EHVPMSM.

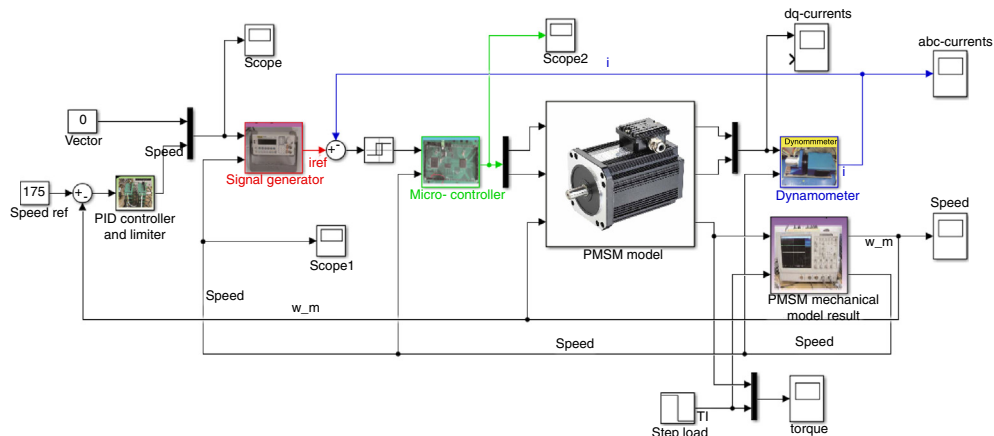


Fig. 7 – Simulink co-simulation architecture for the speed controls of measurements of currents and voltages the simulation configuration of vector control of EHVPMSM of the drive assembly.

current. On the other hand, the component d of the current, which is responsible for the level of flow in the air gap, was set to zero. This was because we had to work in a range of velocities between zero and the nominal machine speed, therefore, it is not necessary to weaken the magnetic flux to work at speeds higher than nominal. Once both current references have been obtained, they will be compared with their measured values. Again, the errors will be introduced in two regulators, the voltage was then returned to the reference voltage. Finally, to close the loop, we needed to measure the current flowing through the three-phase (3-phase) windings and the rotor angle. For this purpose, the Flux Oriented Control (FOC) was chosen. The electric machine designed for the research is an electrical hybrid vehicle of Permanent Magnet Synchronous Machine (EHVPMSM) of 2 kW, 4 poles and smooth rotor. The peculiarity of this engine is its double stator winding. This allows through a series of relays capable of changing the electrical configuration of the windings, connect both stator winding as a single for the pull mode and separate them into two isolated windings (as a transformer) in charging mode. For this project, they were connected to a single winding in the form of a star, since its use only requires the traction mode.

5. Results

5.1. Simulation and experimental results of torque control of EHVPMSM

Sampling results from simulation are shown in Fig. 8 for $100 \mu\text{s}$ of flux reference 0.533 Wb . For the moment at a reference, time of 0.03 s at 2 Nm torque and move to 0.09 s at the same torque 2 Nm , the step change from -3 Nm to 3 Nm . The engine made was a trimmed Siemens brand rotor with ferrite magnets, 1.5 kW , 4 poles, 50 Hz , 380 V nominal voltage and 3.2 A nominal current label with permanent magnet synchronous motors. In Fig. 9 the stator flow response is approximately 0.534 – 0.522 Wb . Flux reference value 0.533 Wb is within this range. In Fig. 10, the vector orbit of the magnetic flux vectors in the form of the flux given in Fig. 11 components seems to be compatible with each other. Figs. 8 and 9 is formed using the de-axial transformation d , q , I and d , q , V graphics. Accordingly, the electromagnetic moment of component q has no contribution to the production and to the d -axis of the moment component current. In Fig. 9, the axis transformation using d , q , V graphics have been obtained. Figs. 9 and 10, it is

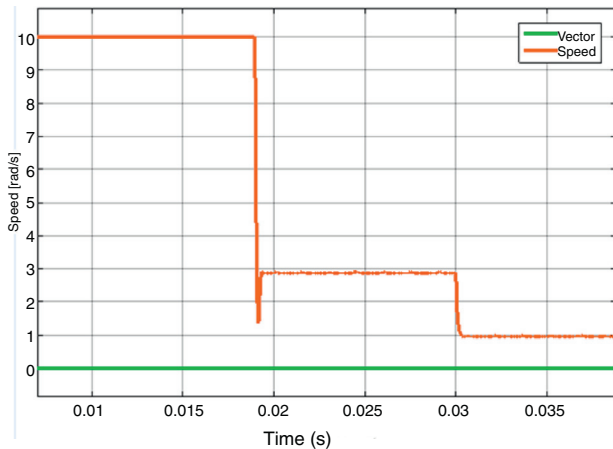


Fig. 8 – Speed and vector of the permanent magnet motor and the winding rotor.

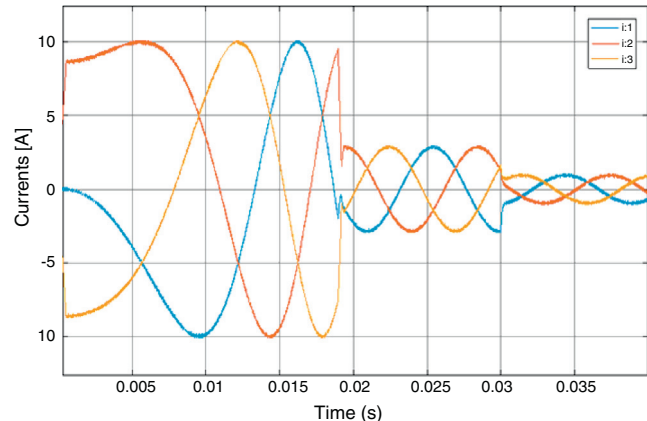


Fig. 11 – Three-phase stator current.

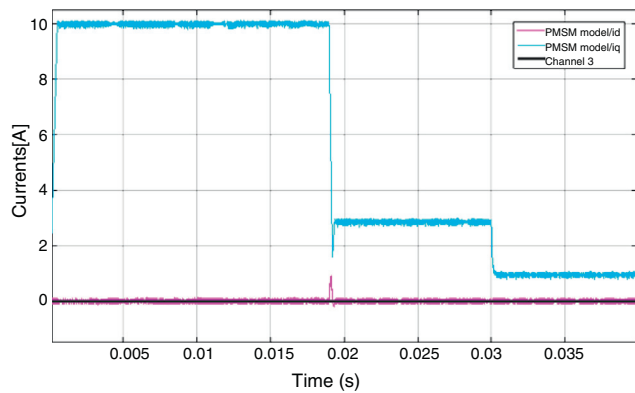


Fig. 9 – Stator currents at start of machine permanent magnet winding rotor of micro-controller of the three function equation of EHVPMSM.

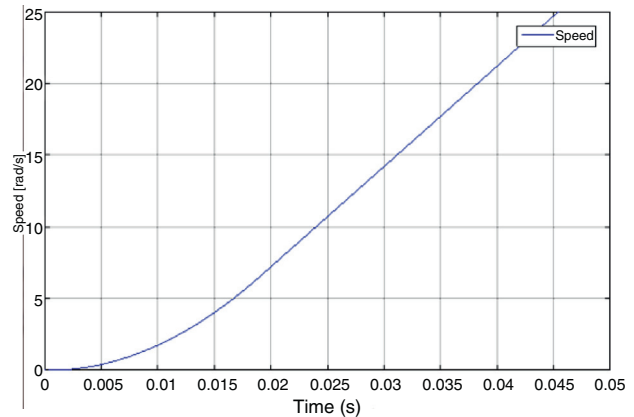


Fig. 12 – stator current of speed from signal generator.

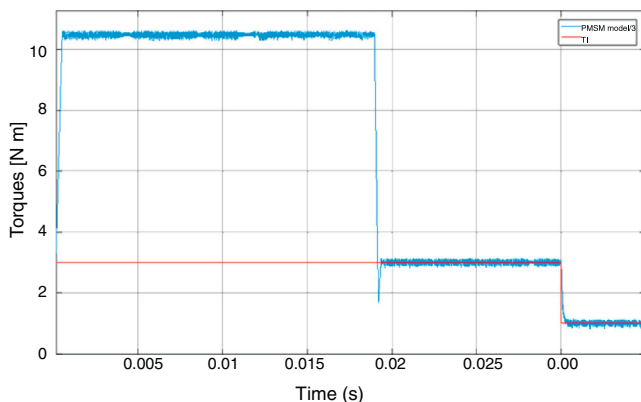


Fig. 10 – Tracking of the permanent magnet motor and the winding rotor technique for EHVPMSM.

seen in the torque response of the torque reference closed. In Fig. 11, a change chart from the square was given. The simulations were performed using a Matlab software. In a file, Matlab data were saved for the engine and controllers and in

Simulink engine, inverter, PWM pulse generation and a three-phase reference system to rotate once and vice versa. For the experiment, two steps were generated in the reference speed with the object to see the dynamic response of the various electrical and mechanical variables of the engine. Fig. 8 shows the motor response to the speed steps. Fig. 10 shows the electrical torque developed by the machine during the simulation. Figs. 9 and 11 show the stator currents during the simulation and a zoom at the time of the step. As can be seen in the graphs, the control system has an “answer fast and accurate” dynamics (Figs. 12–14).

Current and torque error measurement and calculation results are in Table 1, this was obtained from the simulation results. The simulated idle work speed values for all other loaded operating conditions; for the speed error, since it is included in the obtained speed range, no separate columns have been created. The results of the experiment and simulation in Table 1 show the moment, current and speed separately. In simulation, the desired moment value to produce according to the hysteresis band of the driver, $\pm 3.3\% (\pm 0.02 \text{ Nm})$ within the limits. However, from simulation results, the upper and lower limits of the curves should be perceived as the average. The speed results obtained from the simulation are obtained; the speed range from 4010 rpm to 4060 rpm. The only difference is that the engine is idle for 9 m/s

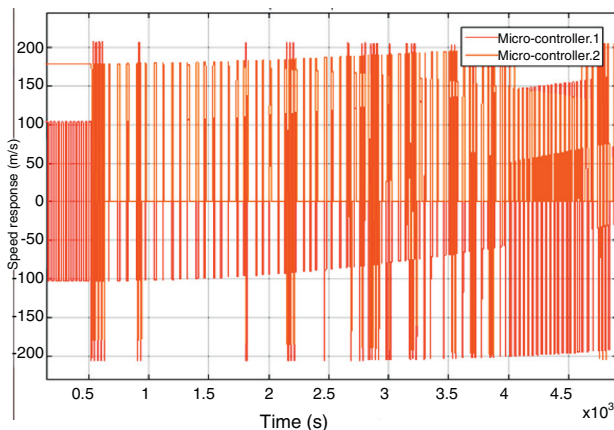


Fig. 13 – Response to the first speed step of micro-controller permanent magnet motor.

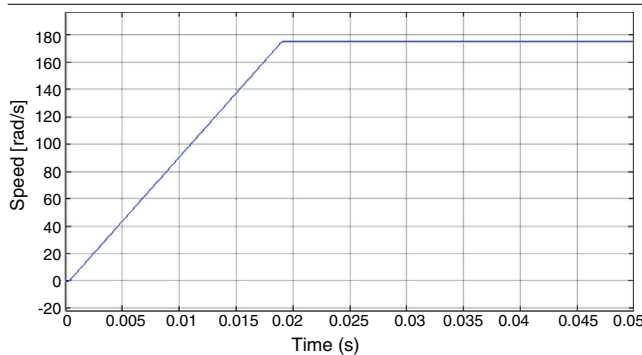


Fig. 14 – Response to the second speed step.

difference in case of operation. This is 0.3% error and its negligible. The motor's nominal power when comparing the current results are close to each other. For example, 0.62 Nm simulation results for torque value the motor phase current is 1.16 A and 1.19 A in the simulation result in [Table 1](#). The difference of

Table 1 – Values of the parameters of the Electric Hybrid Vehicle of Permanent Magnet Synchronous Motor (EHVPMSP) considered in the simulations.

Item	Quantity and unit
Rated voltage (V)	460 V
Power supply (W)	1.1 kW
Rated frequency (f)	50 Hz
Rated torque (T_r)	15 Nm
Stator winding resistance (R_w)	6.1 Ω
Rotor resistance (R_r)	6.01 Ω
Inductance in the directional axis (L_d)	4.2 mH
Inductance in the quadrature axis (L_q)	1.35 mH
Mutual inductance (L_m)	234 mH
Moment of inertial (J)	0.012 kg m^2
Rotor magnetic flux linkage (RMFL) (ψ)	0.21 wb
Number of pole (P_n)	4 pair

0.01 A is 0.7%, which are with the above-mentioned assumptions. In areas near empty work, there is a difference of 0.13 A between the results. These differences are due to the measuring instruments. Because the measured values are measured by the measuring instrument is too far from the maximum measurement value, the measurement was made at a level of 10 A, a lower measurement stage is 0.2 A. Therefore, the results of sensitive measurements in it is open, a maximum of 5.4 A specified on the motor nameplate during the simulations of the current value the entire load is also important that they are not exceeded in the options ([Table 2](#)).

6. Conclusion

In this study, we have been able to establish and investigate direct magnetic synchronous motors moment control with a simulation Simulink/ModelSim was used and experimental validation. The results were compared and a negligible percentage error was obtained. The following conclusion can be drawn from the research work:

Table 2 – Experimental and simulation results.

1. A design simulation and implementation of a novel engine of an Electric Hybrid Vehicle of Permanent Magnet Synchronous Motor (EHVPM) based on field oriented vector control with PID control is proposed.
2. A direct torque control was obtained by adjusting the magnitude and phase angle of the stator flux linkage to match the vector torque required by the load as fast as possible.
3. A new mathematical model was developed for the direct-axis and quadrature-axis of the current to control the speed mechanism for the engine.
4. The battery of the vehicle was charged when connected to the main supply of the EHVPM which eliminates the need for another charging mechanism.
5. The electromagnetic torque of 6.7 Nm was obtained as the maximum torque in 340 μ s. The response of speed transient from -2100 rpm to +2100 rpm in 100 ms of 6.7 Nm torque limit was obtained.
6. A novel way of conserving the energy consumption in a vehicle, which conserves space and weight is simple and reduces cost for industrial application and student learning.

Conflicts of interest

The authors declare no conflicts of interest.

REFERENCES

- [1] Mahmoud MG, Mohammad EB, Mohammad S. Chattering-free sliding mode observer for speed sensorless control of PMSM. *Appl Comput Inform* 2017; <http://dx.doi.org/10.1016/j.aci.2016.12.002>.
- [2] Mahdi Z, Seyed AT, David VM. Neural network-based sensorless direct powercontrol of permanent magnet synchronous motor. *Ain Shams Eng J* 2016;7:729–40.
- [3] Wang Z, Wang C, Qi X, Xianghua M. Study on load torque identification on-line based on vector control of saliency PMSMs. *Procedia Eng* 2011;23:89–94.
- [4] Christianah OI, Bankole IO, Harold MC, Christopher OI. Design and simulation of fatigue analysis for a vehicle suspension system (VSS) and its effect on global warming. *Procedia Eng* 2016;159:124–32.
- [5] Ying-Shieh K, Nguyen VQ, Nguyen TH. Simulink/Modelsim co-simulation and FPGA realization of speed control IC for PMSM drive. *Procedia Eng* 2011;23:718–27.
- [6] Dahlia S, Cyrilraj V, Esther ET. A vehicle control system using a time synchronized Hybrid VANET to reduce road accidents caused by human error. *Veh Commun* 2016;6(October):17–28.
- [7] Muguo L, Da L. A novel adaptive self-turned PID controller based on recurrent-wavelet-neural-network for PMSM speed servo drive system. *Procedia Eng* 2011;15:282–7.
- [8] Gordillo G, Botero AAR, Ramirez EA. Development of novel control system to grow ZnO thin films by reactive evaporation. *J Mater Res Technol* 2016;5(3):219–25.
- [9] Shriwastava RG, Daigavane MB, Daigavane PM. Simulation analysis of three level diode clamped multilevel inverter fed PMSM drive using carrier based space vector pulse width modulation (CB-SVPWM). *Procedia Comput Sci* 2016;79:616–23.
- [10] Rodríguez-Rivas JJ, Peralta-Sánchez E. Design commissioning and testing of an electrodynamometer based on PM synchronous machines. *J Appl Res Technol* 2014;12(June):359–69.
- [11] Hassan AA, El-Sawy AE, Mohamed YS, Shehata EG. Sensorless sliding mode torque control of an IPMSM drive based on active flux concept. *Alex Eng J* 2012;51:1–9.
- [12] <https://www.arrow.com/en/reference-designs/mtrcktsps5604p-3-phase-pmsm-motor-control-development-kit-with-qorivva-mpc5604p-mcu/86eb9dbe0c4a1f3ef0646322dd405812> [retrieved on 29.01.17].
- [13] Behjat V, Hamrahi M. Dynamic modeling and performance evaluation of axial flux PMSG based wind turbine system with MPPT control. *Ain Shams Eng J* 2014;5(4):1157–66.
- [14] Giraldo E, Garces A. An adaptive control strategy for a wind energy conversion system based on PWM-CSC and PMSG. *IEEE Trans Power Syst* 2014;29(3):1446–53.
- [15] Daya JLF, Sanjeevikumar P, Blaabjerg F, Wheeler PW, Ojo JO, Ertas AH. Analysis of wavelet controller for robustness in electronic differential of electric vehicles – an investigation and numerical implementation. *Electr Power Compon Syst* 2016;44(7):763–73.
- [16] Liu JM, Zhu ZQ. Improved sensorless control of permanent magnet synchronous machine based on third-harmonic back-EMF. In: Proc. IEEE International Electric Machines & Drives Conference. 2013. p. 1180–7.
- [17] Qiao Z, Shi T, Wang Y, Yan Y, Xia C, He X. New slidingmode observer for position sensorless control of permanentmagne synchronous motor. *IEEE Trans Ind Electr* 2013;60(February (2)):710–9.
- [18] Rong-Maw J, Chung-Shi T, Ren-Jun L. Robust PID control design for permanent magnet synchronous motor: a genetic approach. *Electr Power Syst Res* 2008;78(7):1161–8.
- [19] Guoyang C, Kemao P, Ben MC, Tong HL. Discrete-time mode switching control with application to a PMSM position servo system. *Mechatronics* 2013;23(8):1191–201.
- [20] Fayed FM, El-Sousy. Adaptive hybrid control system using a recurrent RBFN-based self-evolving fuzzy-neural-network for PMSM servo drives. *Appl Soft Comput* 2014;(21):509–32.
- [21] Jafar K, Parisa D. Fuzzy sliding mode observer for vehicular attitude heading reference system. *Positioning* 2013;4(3):215–26.
- [22] Pierpaolo S, Ion T, Francesca C, Andrea B, Izhak R. Heterogeneous cellular and DSRC networking for Floating Car Data collection in urban areas. *Veh Commun* 2017;8:21–34. ISSN: 2214-2096.